Calibration of an Across Track Interferometric P-Band SAR

Elaine Chapin, Scott Hensley, and Thierry R. Michel

Jet Propulsion Laboratory. MS: 300-235

California Institute of Technology

4800 Oak Grove Drive, Pasadena, CA 91109-8099

Phone: +1 818 354-0497 Fax: +1 818 393-5285 Email: Elaine.Chapin@jpl.nasa.gov

Abstract- The techniques for interferometric calibration of the GeoSAR P-Band system are discussed. These techniques are demonstrated using preliminary GeoSAR data.

I. THE GeoSAR SYSTEM

GeoSAR is an airborne, interferometric Synthetic Aperture Radar (InSAR) system for terrain mapping, currently under development by a consortium including NASA's Jet Propulsion Laboratory (JPL) and Calgis Inc. with funding provided by the National Imagery and Mapping Agency (NIMA). More information about the GeoSAR system can be found in two related papers in this proceedings [1] [2]. The radar simultaneously maps swathes on both sides of the aircraft at two frequencies, X-Band and P-Band. For the P-Band system, the data are concurrently collected for two across track interferometric baselines and at the crossed polarization. The aircraft position and attitude are measured using two Honeywell Embedded GPS Inertial Navigation Units (EGI) and an Ashtech Z12 GPS receiver. The mechanical orientation and position of the antennas are actively measured using a Laser Baseline Metrology System (LBMS). In the GeoSAR motion measurement software, these data are optimally combined with data from a nearby ground station using Ashtech PNAV software to produce the position, orientation, and baseline information used to process the dual frequency radar data.

II. CALIBRATION TECHNIQUE

Proper interferometric calibration of the GeoSAR system is essential to obtaining digital elevation models (DEMs) with the required sub-meter level planimetric and vertical accuracies. Calibration parameters are calculated for each of the four UHF baselines, each of the operational bandwidths (80 and 160 MHz), each transmitted waveform, and each aircraft altitude.

Calibration begins with the determination of the yaw and pitch biases for the two EGI units. To measure the angle biases, the Doppler centroid as a function of range is estimated using the raw range line data. The expected Doppler centroid and the derivatives of the Doppler centroid with respect to an-

gle are calculated given the EGI's measured yaw, pitch, and platform velocity. By comparing the measured and expected Doppler centroids and utilizing the known functional dependence of the difference as a function of angle, the EGI biases can be estimated.

The next stage is the determination of the delays. The differential time delays, the time difference between channels due to different cable lengths, are determined by cross correlating the slant plane images of the channel pairs. Cross correlations can be done throughout the image; no radar identifiable targets are required. The common range delays, the corrections for each mode for unmeasured electrical path lengths in the radar, are solved for concurrently with the platform position error for each pass. The error of the range to a target is given by

$$\frac{\partial \rho}{\partial P_s}\Delta P_s + \frac{\partial \rho}{\partial P_c}\Delta P_c + \frac{\partial \rho}{\partial P_h}\Delta P_h + \frac{\partial \rho}{\partial \tau}\Delta \tau = \Delta \rho, \quad (1)$$

where

$$\frac{\partial \rho}{\partial P_s} = \cos(\beta), \qquad \frac{\partial \rho}{\partial P_c} = \mu \sin(\theta),$$
$$\frac{\partial \rho}{\partial P_h} = -\cos(\theta), \qquad \frac{\partial \rho}{\partial \tau} = 1, \qquad (2)$$

β is the angle between the aircraft velocity and the look direction, θ is the look angle, τ is the common range delay, P_s, P_c, and P_c are the platform position components along track, across track, and vertically, respectively, and

$$\mu = \sqrt{1 - \left(\frac{\cos(\beta)}{\sin(\theta)}\right)^2}. \qquad (3)$$

The location error in range of each target is measured, and equation (1) is solved using singular value decomposition to determine the platform position errors and range error.

Because the antenna locations are measured by the LBMS, baseline calibration consists primarily of measuring a constant offset between mechanical center and the electrical phase center of the antennas. To solve for the baseline and interferometric phase, the error in the position of each target, $\Delta \vec{T}$, is measured. The error is given by

$$\frac{\partial \vec{T}}{\partial B}\Delta B + \frac{\partial \vec{T}}{\partial \alpha}\Delta \alpha + \frac{\partial \vec{T}}{\partial \kappa}\Delta \kappa + \frac{\partial \vec{T}}{\partial \phi}\Delta \phi = \Delta \vec{T}, \qquad (4)$$

where the sensitivity equations used are the same as those that have appeared in the literature except are generalized for the spherical earth and non-broadside imaging [3]. We use singular value decomposition to evaluate a generalized form of equation 4, solving for the error in the baseline length ΔB, the error in the baseline roll angle $\Delta\alpha$, the error in the baseline yaw angle $\Delta\kappa$, and the error in the interferometric phase $\Delta\phi$. Data from multiple passes with different squint angles are synthesized to produce robust estimates of all three components of the baseline.

Calculation of a phase screen, an offset to the interferometric phase difference which is a function of absolute phase and is applied to the interferometric data to compensate for multipath and leakage, is the final calibration stage. The phase screen is calculated by measuring the difference between the measured heights and reference heights from a high resolution DEM over a scene. Height differences at the same absolute phase are averaged together. These height differences are then multiplied by the derivative of the phase as a function of height to calculate a phase offset. The offsets are then fit by a Chebychev polynomial to be used by the processor.

III. CALIBRATION SITE

Our primary calibration site is located in the Santa Lucia Mountain range along the coast of central California in Los Padres National Forest. The ground cover is predominately oak and grassland with open woodland canopies and the closed-canopy of riparian drainages. At the site, 10 large trihedral corner reflectors, 3 large dihedral corner reflectors, and 12 smaller trihedral corner reflectors have been deployed for GeoSAR calibration. Most of the reflectors are arranged in an approximate line across track, but two are separated along track and two are viewed by the opposite look direction. Simultaneously imaging corner reflectors on both sides of the aircraft greatly improves our estimates of the common range delays and the platform position error. Figure 1a shows an image of calibration area. The across track line of corner reflectors are positioned in the dark, flat, grassy area near the center of the image. There is approximately 800 m of relief over the full calibration site as can be seen in Figure 1b.

Figure 1c is an image of the statistical height error for each of the 5 by 5 m pixels. The statistical height errors vary from 0 to 300 cm over the full 17.4 km swath. The statistical height error is larger in the far range than the near range and is larger in areas where the backscatter image is dark.

One difficulty in P-Band interferometric calibration and validation is determining the correct heights to compare with the height maps produced by the P-Band interferometer. One of the goals of the GeoSAR program is to study P-Band penetration into various types of vegetation. If the scene imaged is covered with vegetation, is the correct altitude the true ground surface, the top of the trees, or somewhere in between? If the scene has no vegetation, the signal to noise ratio can be low resulting in noisy height estimates and unwrapping difficulties.
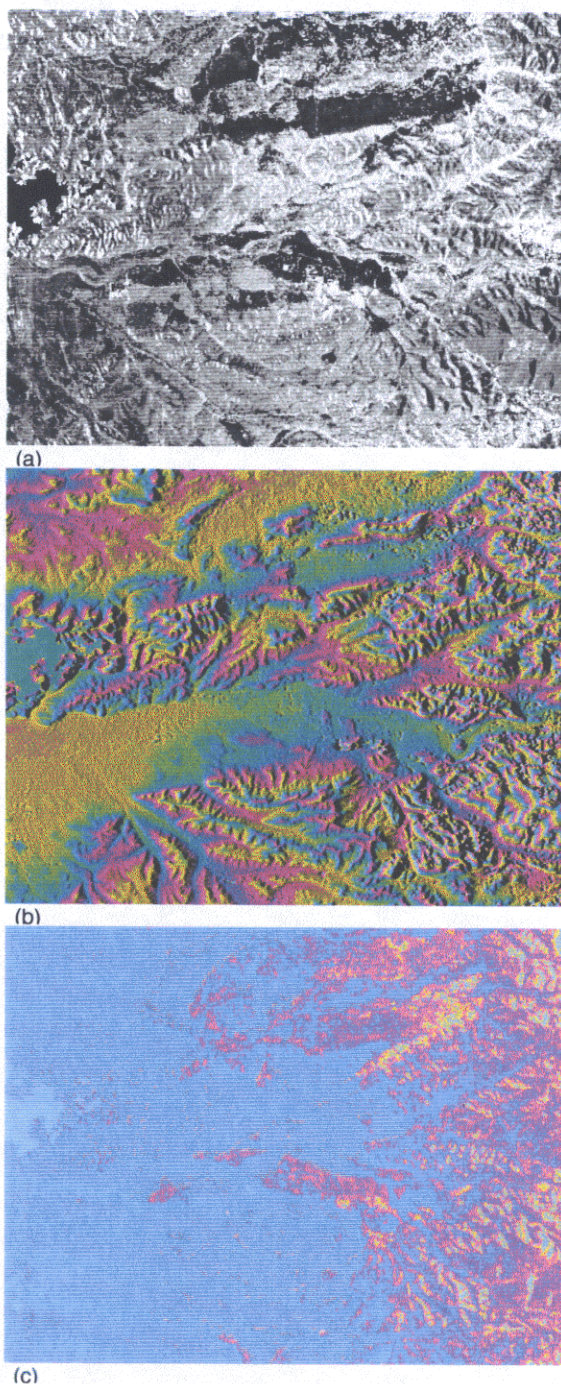

(a)

(b)

(c)

Fig. 1. (a) Radar backscatter image of entire calibration area. The area mapped is approximately 17.4 km across track and 14 km along track. North is towards the bottom right. (b) Shaded relief image overlaid on P-Band derived DEM shown over entire calibration area. The colors for the height repeat every 100 m. (c) Image of the statistical height error of each mapped pixel. Errors vary from 0 to 300 cm over the full image.

Because water decorrelates during the long P-Band aperture length, ocean surfaces can not be used for P-Band calibration the way they are for higher frequency radars. The perfect site for determining a P-Band phase screen would have no vegetation but would be rough at P-Band scale sizes.

IV. EXAMPLE P-BAND CALIBRATION

The calibration software has been exercised on several of our preliminary data sets, and in this section we will provide an example. Figure 2 shows a radar backscatter image of a small portion of our radar calibration site. The data shown was collected in the low resolution 80 MHz bandwidth mode and was processed using the ping-ponged baseline. The bright area in the lower center of the image is a clump of oak trees on a small hill. The dark area on the right side of the image is a grassy area dotted man made structures. The bright dots in dark areas of the image are isolated oak trees and corner reflectors. A careful examination of Figure 2 reveals that the height measured at each of the isolated oaks is slightly higher than the surrounding grassy areas. The bright band crossing the top of the image is the trees growing along the San Antonio river.

A common range delay, a baseline correction, a differential time delay, and a differential phase delay were calculated for the data shown in Figure 2. Figure 3 shows the errors in the corner reflector positions before and after these calibration parameters were calculated.

ACKNOWLEDGMENT

REFERENCES

[1] S. N. Madsen, "Motion Compensation of UWB SAR", *IGARSS Proc. 2001*.

[2] S. Hensley, E. Chapin, A. P. Freedman, C. Le, S. N. Madsen, T. R. Michel, E. Rodríguez, P. R. Siqueira, and K. Wheeler, "First P-band results using the GeoSAR mapping system", *IGARSS Proc. 2001*.

[3] P. A. Rosen, S. Hensley, I. R. Joughin, F. K. Li, S. N. Madsen, E. Rodríguez, and R. M. Goldstein, "Synthetic aperature radar interferometry," *Proc. IEEE*, vol. 88, no. 3, pp. 333-382, 2000.
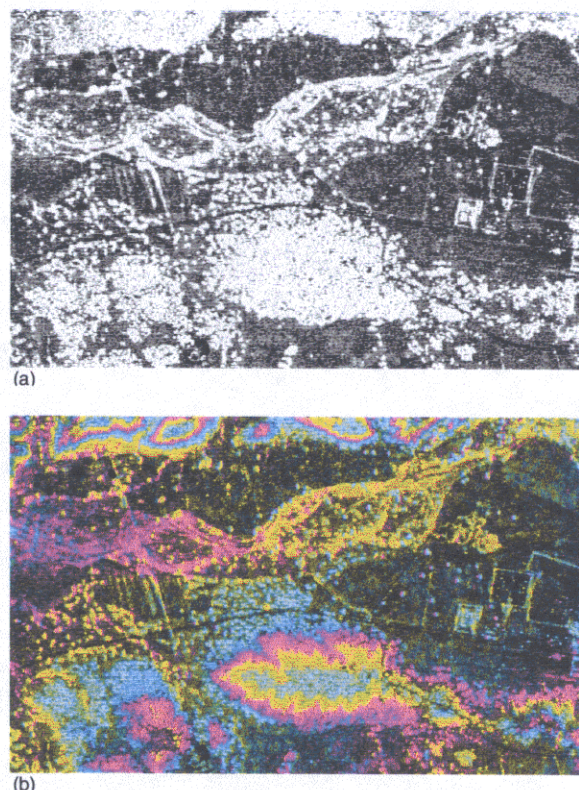
Fig. 2. (a) Radar backscatter image of a clump of oak trees and riparian environment near the San Antonio river near the center of our calibration site. The area mapped is approximately 3.7 by 2.3 km. North is towards the bottom right. (b) Radar backscatter shown over the P-Band derived DEM. The colors for the height repeat every 30 m.
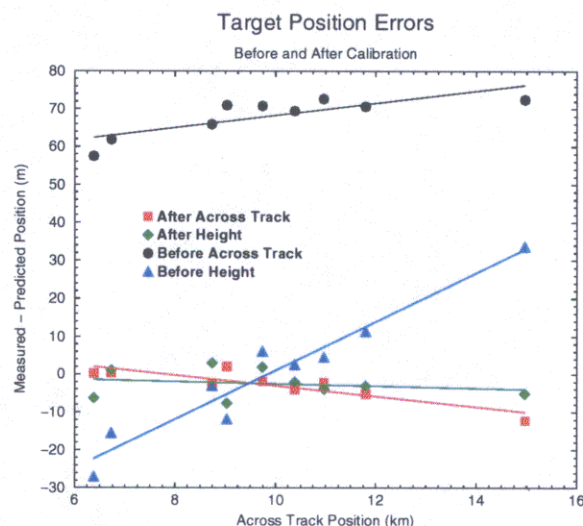

Fig. 3. Corner reflector position errors before and after calibration